Chapter 1

Introduction

Seismic anisotropy in complex earth subsurface has become increasingly important in seismic imaging due to the increasing offset and azimuth in modern seismic data. To account for anisotropic wave propagation, sophisticated wave extrapolation and imaging techniques have been developed for subsurface areas that are as complex as orthorhombic media. However, building an accurate and reliable anisotropic earth model remains a challenge to the seismic industry due to its nonlinear and underdetermined nature. This thesis presents an automated, wave-equation-based anisotropic model building methodology that integrates surface seismic data, geological information, and prior rock physics knowledge of the subsurface.

EARTH MODEL BUILDING

Subsurface models, including both the background wave-speed model and the structural image, are essential for interpretation, drilling and reservoir modeling. In this thesis, I aim to build a reliable wave speed model that enables the creation of an accurate structural image of the subsurface.

Isotropy or anisotropy

In the seismic-exploration industry, seismic wave speed models are widely needed to explain the travel time of the recorded data. Seismic waves travel in heterogeneous media at different speeds in different directions. This directional dependence of the seismic wave speed is usually referred to as *seismic anisotropy*. Although seismic anisotropy was reported in exploration seismology in the 1930s (McCollum and Snell, 1932; Postma, 1955; Helbig, 1956), it did not play a significant role in seismic imaging until the 1980s. However, as seismic exploration develops to more complex geology and deeper targets, the necessity of including seismic anisotropy has been recognized. Modern seismic acquisition is performed with long offsets (sometimes with more than 10 km) and full azimuthal coverage. Consequently, the data collected recently are highly sensitive to anisotropy and cannot be explained by simple isotropic models.

To account for the kinematic effects of anisotropy, various wave extrapolation schemes have been developed for subsurface models that are as complex as orthorhombic media (Shan, 2009; Fletcher et al., 2009; Zhang and Zhang, 2009; Fei and Liner, 2008). However, the most common anisotropic model in seismic imaging and model building is still the transverse isotropic (TI) model. The TI model is the simplest anisotropy model, and it is a reasonable approximation for many sedimentary environments in the subsurface.

Figure 1.1 shows two different types of TI models: the vertical transverse isotropy (VTI) and the tilted transverse isotropy (TTI). For P-wave, the wave speeds in the transverse plane are the same, but the wave speed in the perpendicular direction is different. When the symmetry axis is vertical, the vertical velocity v_v, horizontal velocity v_h, and normal moveout (NMO) velocity v_n, are all needed to define the P-wave wavefront in a homogeneous VTI medium (Tsvankin and Thomsen, 1994; Alkhalifah and Tsvankin, 1995). When the symmetric axis is tilted, the dip angle θ and the azimuth angle α, are also needed to determine the symmetry axis. In my thesis study, I focus on the VTI model because it is the most needed anisotropic model for seismic imaging, and it is sufficient to characterize most of the shale-rich

sedimentary basins in the Gulf of Mexico.

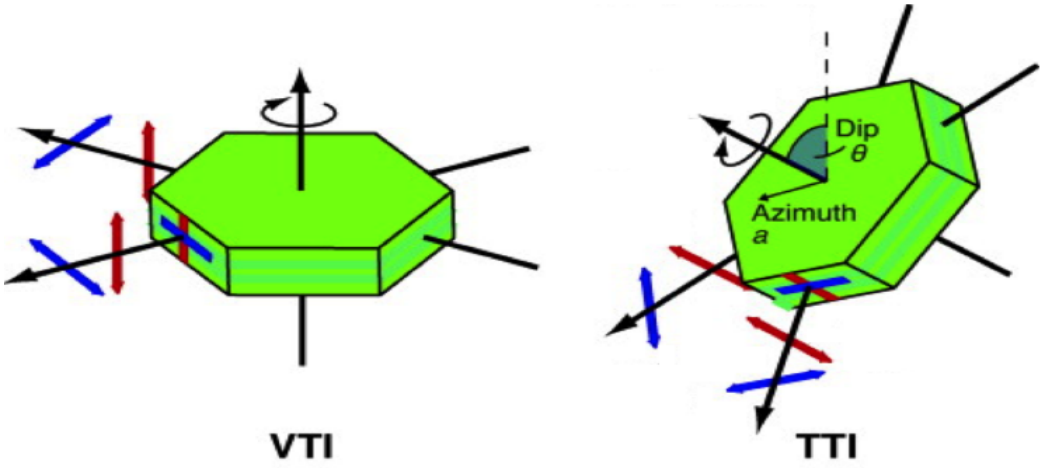

Figure 1.1: Left: A sketch of the wave-speed symmetry for VTI medium. Right: A sketch of the wave-speed symmetry for TTI medium. [**NR**] chap1/. timedia

Thomsen (1986) introduced dimensionless parameters that relate the three velocities in a TI medium as follows:

$$v_h^2 = v_v^2(1 + 2\epsilon), \tag{1.1}$$

$$v_n^2 = v_v^2(1 + 2\delta). \tag{1.2}$$

Parameters ϵ and δ define the degree of anisotropy of a medium. The medium is isotropic when $\epsilon = \delta = 0$.

Figure 1.2 shows the comparison of wavefronts propagated from a point source in both isotropic and VTI media. The traveltime from the source to the wavefront is 1 sec. The solid line shows the (semi-)circular wavefront in an isotropic medium; the dashed line shows the (semi-)elliptical wavefront in a VTI medium with $\epsilon = \delta = 0.2$; and the dotted line shows the wavefront in a VTI medium with $\epsilon = 0.2$ and $\delta = -0.2$. The positive ϵ leads to the advanced wavefront in the horizontal direction compared with the isotropic wavefront. The positive or negative δ determines the faster or

slower velocity in the near-vertical direction compared with the vertical velocity.

The differences between both the VTI wavefronts and the isotropic wavefront are small when the propagation direction is within 20° around the vertical. The differences between the $\epsilon = \delta = 0.2$ wavefront and the isotropic wavefront become more apparent as the propagation direction deviates from vertical. Tradeoff effects can be seen from the dotted wavefront when $\epsilon = 0.2$ and $\delta = -0.2$. The positive ϵ effect has been compensated by the negative δ effect. Because the vertical velocity is the same, the differences between the dotted wavefront and the isotropic wavefront are rather small when the propagation direction is within 60° around the vertical. The differences only become significant when the propagation angle is greater than 60°. Therefore, presence of dipping reflectors and/or long offset acquisition will magnify the anisotropic effects.

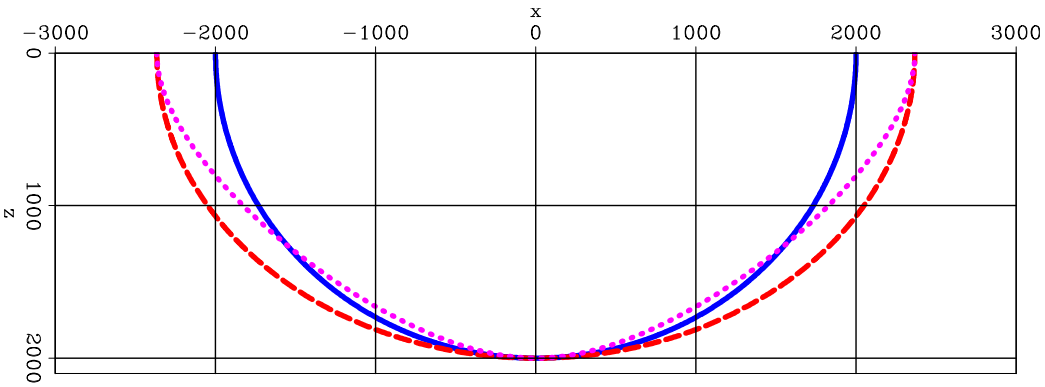

Figure 1.2: Comparison of wavefronts propagated from a point source at $x = 0$, $z = 0$ in homogeneous isotropic and VTI media. Parameters used to propagate the wavefronts are: $\epsilon = 0$ and $\delta = 0$ for the solid line; $\epsilon = 0.2$ and $\delta = 0.2$ for the dashed line; and $\epsilon = 0.2$ and $\delta = -0.2$ for the dotted line. The vertical velocity of the medium is 2000m/s in all three cases. [**ER**] chap1/. vtiwavefronts

Alkhalifah and Tsvankin (1995) introduced the anellipticity parameter η which directly relates v_h with v_n as follows:

$$v_h^2 = v_n^2(1 + 2\eta), \tag{1.3}$$

with

$$\eta = \frac{\epsilon - \delta}{1 + 2\delta}. \tag{1.4}$$

The parameter η describes the anellipticity of the wavefront. When $\eta = 0$, the wavefront is an ellipsoid, and the medium is elliptical anisotropic. Alkhalifah and Tsvankin (1995) showed that v_n and η are the only two parameters that determine the long-spread (nonhyperbolic) P-wave moveout assuming horizontal reflectors.

Now we have six parameters to describe the VTI media, but only three are independent. In this thesis, I refer to any three-parameter combination which fully describes a VTI medium as a *VTI model*, and its components as the *VTI parameters*. I refer to the dimensionless parameters ϵ, δ, and η as the *anisotropic parameters*. Based on the available information, only a subset of the three VTI parameters can be reliably resolved.

Ray-based or wave-equation-based tomography

The state of the art in anisotropic model building is represented by ray-based tomography (Woodward et al., 2008). Ray-based methods are efficient and adequate in relatively simple geological settings with mild velocity contrasts. However, they often fail to describe the complexity of the wave propagation due to its infinite-frequency approximation. Figure 1.3 shows the comparison between a snapshot of the traced rays and a snapshot of the wavefields. The ray approximation over simplifies the wavefields above the salt body and fails to model the complex transmitted wavefronts through the salt body.

Furthermore, the sensitivity kernels for velocity and anisotropy are frequency dependent (Woodward, 1992). To capture the frequency-dependence of the model sensitivity, we should back project the model updates along the band-limited wavepaths rather than the infinite-bandwidth rays.

To overcome the limitations of ray-based tomography, many wave-equation-based tomography methods (known as wave-equation migration velocity analysis (WEMVA))

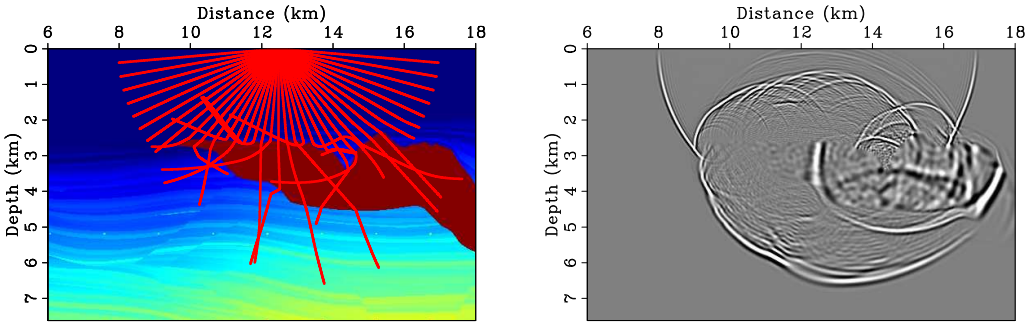

(a) (b)

Figure 1.3: Comparison between rays and wavefields. Panel (a) shows a snapshot of the rays overlaid by the Sigsbee2A velocity model, (b) shows a snapshot of the wavefields. [**ER**] chap1/. sigsb2a-rays-vmod,sigsb2a-wave-snapshot

(Biondi and Sava, 1999; Sava and Biondi, 2004a,b; Shen and Symes, 2008) were proposed to use the wavefields as information carriers. These methods work in the prestack image space and utilize the incoherency with reflection angle or data offset in the image gathers to update velocity. Figure 1.4 shows an example of the different moveouts in the angle domain common image gathers (ADCIGs) when different velocity models are used in imaging. The ADCIGs are flat (Panel (b)) when the migration velocity is accurate. When the migration velocity is lower or higher than the true velocity, the ADCIGs show upward or downward residual moveouts, respectively (Panel (a) and (c)). The WEMVA algorithms then translate the residual moveouts into model updates and improve the background velocity model.

We can apply the same criteria to evaluate the accuracy of the anisotropic parameters ϵ and δ. Figures 1.5 and 1.6 show the ADCIGs when different anisotropic parameters are used for imaging (while the other VTI parameters are accurate). We observe similar moveout patterns for the anisotropic parameters as for velocity. However, the absolute moveouts (depth differences from zero angle) with respect to 50% perturbation in the anisotropic parameters are much smaller than that with respect to 5% perturbation in the vertical velocity (Figure 1.4). This suggests the WEMVA objectives have much lower sensitivities for anisotropic parameters than for velocity.

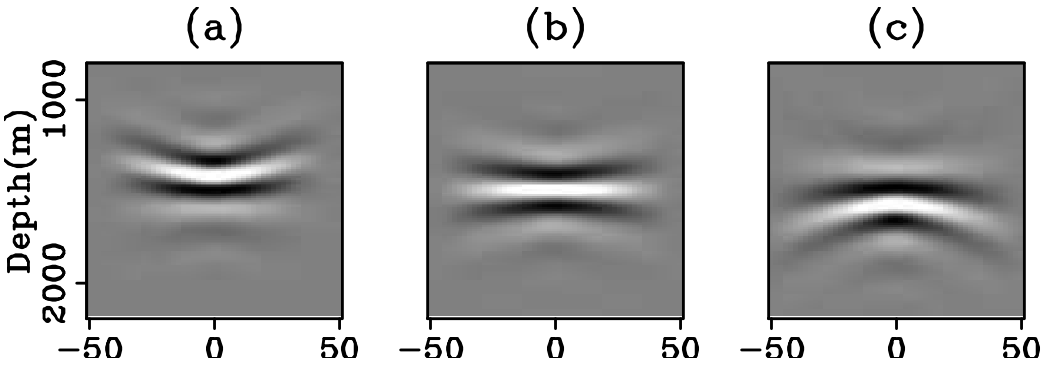

Figure 1.4: Angle domain common image gathers with (a) 5% slower velocity, (b) accurate velocity, and (c) 5% faster velocity. [**CR**] chap1/. aimg-vel

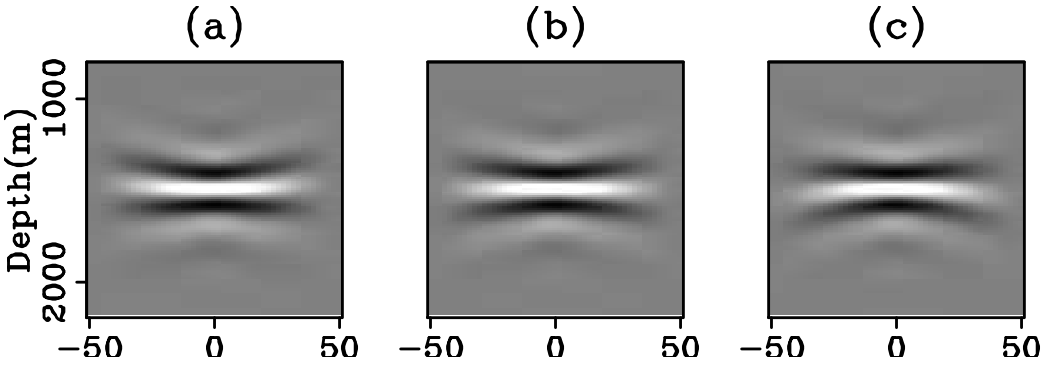

Figure 1.5: Angle domain common image gathers with (a) 50% smaller ϵ, (b) accurate ϵ, and (c) 50% larger ϵ. [**CR**] chap1/. aimg-eps

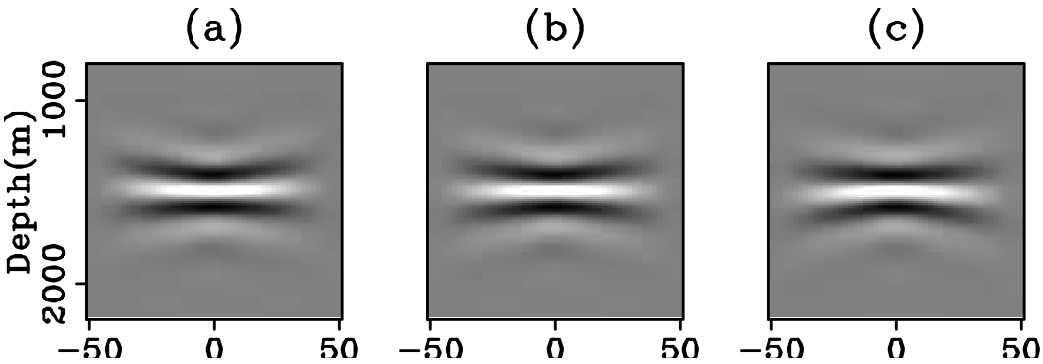

Figure 1.6: Angle domain common image gathers with (a) 50% smaller δ, (b) accurate δ, and (c) 50% larger δ. [**CR**] chap1/. aimg-del

Data integration

Earth model building is an underdetermined and hence challenging inverse problem, especially at the exploration stage. In general, the input information can be obtained from geological information, surface seismic data, and rock physics modeling from well logs. During early exploration, the geological information often comes from plate or regional tectonics to identify the potential target area. Surface seismic data are acquired to image the structure of the subsurface after establishing the area of interest. Based on the preliminary interpretation results, a few exploration wells will be drilled to verify the earth model. The initial model building results are often far from the true subsurface. Therefore, corrections of the earth model by integrating all available information is necessary.

Surface seismic data have the best compromise between accuracy and coverage among the three types of information. Geological knowledge covers large regions without accurate positions, whereas well logs provide accurate, high resolution information only at sparse locations. Therefore, most of the current practices of information integration occur after seismic imaging and structural interpretation. First, seismic images are stretched vertically according to the well markers. Then, borehole core analysis is propagated from the well location to the rest of the region based on

the seismic images and the underlying geological assumptions. However, this conventional workflow does not include a feedback loop to verify if the modified seismic images honor the original seismic data. Therefore, inconsistencies may be introduced by the sequential evaluations of the data.

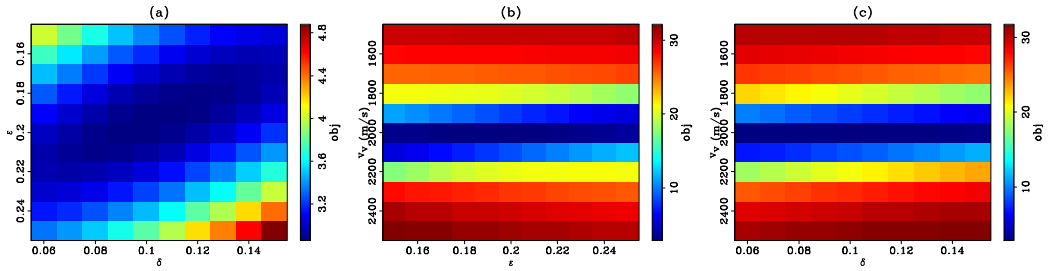

Figure 1.7: WEMVA objective function with respect to (a) ϵ and δ, (b) vertical velocity and ϵ, and (c) vertical velocity and δ. The third parameter is accurate on each panel. Notice the different color scale in panel (a). [**CR**] chap1/. objfun1

Simultaneous integration of different data types becomes essential when the earth model becomes more complex. With the increasing number of unknowns at each subsurface location, the model building problem based on a single type of data becomes more non-linear and underdetermined.

For example, Figure 1.7 plots the WEMVA objective function based on the surface seismic data with respect to a range of the model parameters. This objective function evaluates the coherence in the ADCIGs when different model parameters are used to migrate the surface seismic data (such as in Figures 1.4, 1.5, and 1.6). The WEMVA objective function can resolve the vertical velocity accurately regardless of the accuracy of the anisotropic parameters. However, it cannot correctly resolve the anisotropic parameters when the vertical velocity is inaccurate. Even when the vertical velocity is accurate, the nearly flat objective function in the ϵ-δ space (Figure 1.7(a)) suggests that the WEMVA objective function cannot sufficiently constrain the anisotropic parameters.

Moreover, severe tradeoffs among the VTI parameters are shown in the objective function plots. A strong tradeoff can be seen in Figure 1.7(a). The WEMVA

objective function cannot resolve ϵ or δ independently as long as the summation of the two remains the same (unless events propagating at more than 60° angles are recorded), as has been observed from the wavefronts in Figure 1.2. Tradeoffs between the anisotropic parameters and the vertical velocity can also be seen from Figures 1.7(b) and 1.7(c), where positive vertical velocity errors are compensated by negative errors in the anisotropic parameters and vice versa. Nevertheless, these tradeoff effects are much less obvious, further demonstrating the low sensitivity of seismic data to the anisotropic parameters.

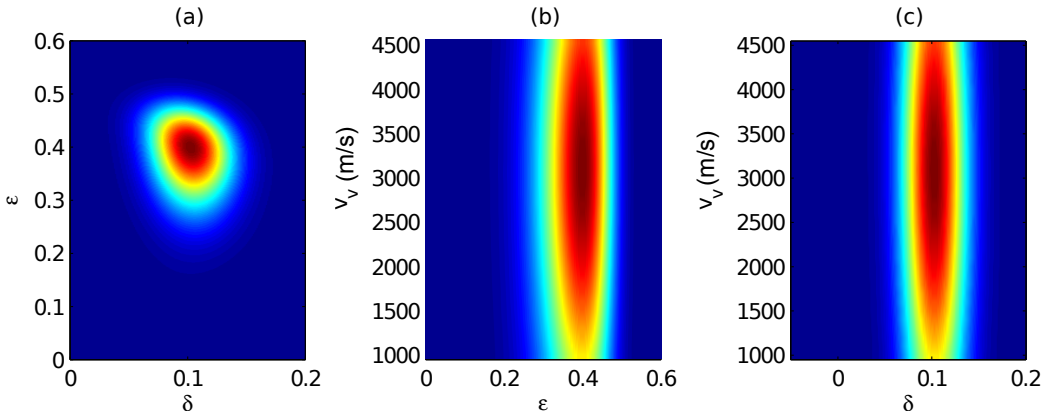

Figure 1.8: Stochastic rock physics modeling results for parameters v_v, ϵ and δ. [**ER**] chap1/. rockphy

On the other hand, our prior knowledge suggests that the VTI parameters are correlated with each other. Locally, the lithology determines the correlation/covariance among the VTI parameters. These correlations can be measured by stochastic rock physics modeling using the well logs as input (Bachrach et al., 2011). Figure 1.8 shows the rock physics objective function based on a compacting shale model. Compared to the WEMVA objective function (Figure 1.7), the rock physics objective function has much looser control of velocity, suggesting similar lithology can result in a wide range of seismic velocities. In contrast, the rock physics objective function defines a much tighter possible range for anisotropic parameters ϵ and δ. These lithological-based distributions can be summarized as a cross-parameter covariance.

Spatially, the correlations of the parameters are defined by the geological model in the sedimentary basin. In a compaction-based model, the wave speeds vary smoothly parallel to the sea bottom (e.g., Slotnick (1936); Kaufman (1953)). In a lithology-based model, the wave speeds follow the structural dip (Clapp, 2000; Woodward et al., 2008). The anisotropic parameters, being the ratio between the wave speeds, are often considered spatially smoother than the wave speeds themselves. These spatial correlations of each parameter can be summarized as the spatial covariance based on the underlying geological models.

Surface seismic data, rock physics modeling from the well logs, and the geological models each define the VTI parameters from different prospectives and provide complementary information for each other. Therefore, the focus of this thesis is to define effective methods which intelligently combine all information to produce a coherent and consistent model is the focus of this thesis.

OVERVIEW OF THESIS

The goal of this thesis is to integrate different sources of information about the subsurface at different scales in order to produce a reliable anisotropic subsurface model that is consistent with all the available information.

WEMVA for VTI models

In Chapter 2, I extend the concept of wave-equation migration velocity analysis (WEMVA) to anisotropic media. I define the anisotropic WEMVA objective function in the image space by evaluating the flatness of the angle domain common image gathers and the focusing (stacking power) of the stacked image. I derive the gradients of the WEMVA objective function with respect to the VTI parameters and reparameterize the inversion using NMO velocity v_n and the anellipticity parameter η due to the lack of complementary information. I introduce a regularization term to include the geological information into the inversion.

Using both a synthetic and a field data example, I show how anisotropic WEMVA can identify localized anomalies in both NMO velocity and the η model. On the synthetic data, I show that anisotropic WEMVA improves the flatness in the angle domain common image gathers and corrects for the positioning error due to the velocity and η anomalies. On the field data, I show that anisotropic WEMVA improves the resolution of the stacked image and enhances the definition of a major fault in the 2D section.

Anisotropic WEMVA with rock physics constraints

In Chapter 3, I build the framework to regularize the wave-equation tomography that utilizes the available geological and rock physics information. I use the geological information to approximate the spatial covariance for each individual parameter and the rock physics information to approximate the multi-parameter covariance at a particular location. From a simple missing data problem, I demonstrate the extra information the cross-covariance (cross-correlation) among the VTI parameters contributes to the inversion.

On a synthetic example, I compare and contrast the inversion behaviors of the anisotropic WEMVA when three different rock physics covariance matrices are applied. I show that the additional rock physics information will not change the solution of the inversion problem for the well-constrained parameter. Nevertheless, additional rock physics information improves the convergence and the resolution of the well-constrained parameter during the early iterations. By comparing and contrasting the inversion results, I show that the rock physics information is essential to resolve the less-constrained parameters. I show that, the anisotropic WEMVA successfully improves the focusing and the positioning of the migration image in all three inversion tests.

Field data tests

In Chapter 4, I apply the anisotropic WEMVA with geological and rock physics constraints to a 3D dataset from the Gulf of Mexico. I construct the rock physics covariance at every grid point in the model space based on the well logs and the previously interpreted seismic results. Based on the rock physics modeling results, I show that the general trends of velocity-anisotropy correlation are positive in the shallow region, but become negative when the mineral transition of the shales become the dominant factor for both velocity and anisotropy.

I invert the seismic data acquired by an ocean-bottom-system using the proposed anisotropic WEMVA methodology. The inversion results improve both focusing and resolution of the migrated images.

Appendices

In Appendix A, I describe the optimization-based implicit finite differencing scheme I use to extrapolate the wavefield. The optimized coefficients and their derivatives are further used when differentiating the wave-equation with respect to the anisotropic parameters.

In Appendix B, I provide the details for the rock physics models I use to model the compaction-induced shale anisotropy and thin-layering-induced anisotropy in Chapter 4. I show how the previous interpretation results can be used to construct the rock physics covariance matrix in space.

In Appendix C, I provide a synthetic example of the anisotropic WEMVA based on reverse time migration (RTM). RTM handles the large-angle propagation better than one-way wave-equation migration (WEM). However, I keep the one-way WEM implementation in my thesis study to maintain a low computational cost and thus to be able to test the method on 3D dataset, given the computational resource available for this project.

ASSUMPTIONS AND LIMITATIONS

Model assumption is one of the weaknesses of the method presented in this thesis. Although the VTI model can sufficiently describe many geological scenarios, it may not adequately explain formations with steep dips or layered media with one or multiple sets of fractures. More complex models (TTI or orthorhombic model) with more parameters are needed to fully characterize the P-wave propagation. In those cases, the concept of constraining the model building process using the rock physics covariance is even more valuable because the inversion will be more underdetermined with stronger ambiguities among the parameters.

The second assumption comes from the rock physics models. Although I capture the uncertainties in the rock physics modeling through a stochastic modeling process, the additional information I introduce into the inversion is as accurate as the rock physics modeling. The geological and lithological scenarios are limited by the ranges of the rock physics models. However, when in doubt, we can reduce the strength of the rock physics constraints by changing the value of the trade-off parameter for the regularization.

Finally, the resolution and accuracy of the inversion presented in this thesis is limited by the fact that we ignore the presence of shear waves. Although the signal-to-noise ratio of shear wave is usually lower than that of pressure wave, shear waves are more sensitive to the anisotropic properties of the subsurface. Therefore, jointly inverting pressure and shear waves with proper constraints may produce better solutions to the anisotropic model building problem.